J Geod (2007) 81:213–230
DOI 10.1007/s00190-006-0102-4

ORIGINAL ARTICLE

An improved and extended GPS-derived 3D velocity field of the glacial isostatic adjustment (GIA) in Fennoscandia

Martin Lidberg · Jan M. Johansson · Hans-Georg Scherneck · James L. Davis

Received: 3 October 2005 / Accepted: 6 September 2006 / Published online: 17 October 2006

Abstract We present a new GPS-derived 3D velocity field for the Fennoscandia glacial isostatic adjustment (GIA) area. This new solution is based upon ∼3,000 days of continuous GPS observations obtained from the permanent networks in Fennoscandia. The period encompasses a prolongated phase of stable observation conditions after the northern autumn of 1996. Several significant improvements have led to smaller uncertainties and lower systematic errors in the new solutions compared to our previous results. The GPS satellite elevation cut-off angle was lowered to 10°, we fixed ambiguities to integers where possible, and only a few hardware changes occurred over the entire network. The *GAMIT/GLOBK* software package was used for the GPS analysis and reference frame realization. Our new results confirmed earlier findings of maximum discrepancies between GIA models and observations in northern Finland. The reason may be related to overestimated ice-sheet thickness and glaciation period in the north. In general, the new solutions are more coherent in the velocity field, as some of the perturbations are now avoided. We compared GPS-derived GIA rates with sea-level rates from tide-gauge observations, repeated precise leveling, and with GIA model computations, which showed consistency.

M. Lidberg (✉) · J. M. Johansson · H.-G. Scherneck
Onsala Space Observatory,
Chalmers University of Technology,
439 92 Onsala, Sweden
e-mail: lidberg@oso.chalmers.se

J. L. Davis
Harvard-Smithsonian Center for Astrophysics, Cambridge, MA, USA

Keywords Glacial isostatic adjustment (GIA) · Postglacial rebound (PGR) · Global Positioning System (GPS) · Terrestrial reference frame (TRF) · ITRF2000 · GAMIT/GLOBK software · Fennoscandia

1 Introduction

The land uplift, postglacial rebound (PGR) or glacial isostatic adjustment (GIA) (now commonly termed the latter) process in Fennoscandia has been a subject of scientific research for more than a century (e.g., Ekman 1991; Frängsmyr 1976). It is now recognized to be part of the global process of GIA, which originates from the last glacial cycle culminating about 20,000 years ago. When the load from the ice (thickness of about 2–3 km) was removed, the Earth responded as a viscoelastic body, resulting in vertical – as well as horizontal – displacements towards a new equilibrium (e.g., Milne et al. 2001).

A wide variety of geophysical and geodetic observable features and quantities have been exploited to study the GIA process. This includes tide-gauge records, repeated geodetic leveling, gravity anomalies, changes in gravity, and time series of ancient sea level elevations. These are, in a geometrical sense, primarily related to the vertical component. They are also not observations of absolute change of the Earth's crust but relative, e.g., where a tide gauge measures the height of the sea relative to the land (in the short term) or the height of the land relative to sea level (in the long term).

The late 1980s and early 1990s witnessed a rapid development in space geodesy, evolving predominantly around the Global Positioning System (GPS): the

constellation became complete, receiver design advanced, and equipment and post-processing costs dropped. Analysis techniques also developed, including the International GNSS (Global Navigation Satellite Systems) Service (IGS). By means of the IGS, geodetic positions obtained from GPS are related to a global geocentric coordinate system. Time series of daily GPS positions from a network of GPS stations may be used to infer a bundle of displacement vectors, sampling the 3D deformation field.

In 1993, the Baseline Inferences for Fennoscandian Rebound Observations Sea Level and Tectonics (BIFROST) project was started, with a primary goal to establish a new and useful 3D measurement of movements of the Earth's crust in this region, able to constrain models of the GIA process in Fennoscandia. A network of permanently operating GPS receivers was established in Sweden and Finland at an inter-station distance of 100 to 200 km. A comprehensive description of the BIFROST project, including data analysis and results from August 1993 to May 2000, is presented in Johansson et al. (2002) and Scherneck et al. (2002). The first years (until the northern autumn of 1996) covered in these solutions was a period of intensive development, e.g., changes of the antenna protective covers (radomes), and repeated checks of monument stability, which resulted in frequent disturbances in the antenna environment and thus "jumps" in the GPS time series.

In this study, which is a part of the BIFROST effort, we have analyzed GPS observations from January 1996 until June 2004. This period covers 8.5 years compared to 6.5 years for the previous published BIFROST solutions. This extended period has been stable with few changes or management events regarding GPS antenna installation or monumentation, thus resulting in an increased length of uninterrupted periods in the time series from typically 4.5 to 7.5 years.

We have also extended the network of GPS stations spatially so as to cover peripheral areas of the GIA process. This strategy may eventually help in determining the part of the Eurasian tectonic plate affected by intra-plate deformation due to the GIA process. The GPS data analysis has also been improved by reducing the elevation cut-off angle from 15° to 10° strengthening, in particular, the vertical component of the solution, and we solve for integer carrier-phase ambiguities in the GPS observations.

2 The extended BIFROST GPS network

The BIFROST GPS network is composed of the permanent GPS network of Sweden (*SWEPOS*™, SWEPOS (2005)/*online*/) and Finland (*FinnRef*®, FGI (2005)/*online*/) (Johansson et al. 2002; Koivula et al. 1998; Scherneck et al. 2002). This study also includes permanent GPS stations in Norway (*SATREF*®, SATREF 2005/*online*/) and Denmark that contribute to the EUREF Permanent Network (EPN; cf. Panafidina et al. 2006) as well as a selection of EPN stations in Northern Europe. Detailed information about the EPN stations may be found at the EPN web page (EUREF 2005/*online*/).

By including stations in the outer area of the Fennoscandian GIA process, we may eventually be able to determine the area of the Eurasia tectonic plate, where intra-plate deformation due to GIA must be taken into account, given a specific accuracy level. The additional stations are also needed for the reference frame realization, where the extended BIFROST network is combined with networks from global analysis (see Sect. 3). The location of the BIFROST stations is displayed in Fig. 1, where the four-character site identifications are those recognized by the IGS, the EPN, or the respective national GPS services.

3 Data analysis

3.1 Analysis of GPS data

In this study, we have used the *GAMIT/GLOBK* software package version 10.1 (King 2002; King and Herring 2002), developed at the Massachusetts Institute of Technology (MIT), Scripps Institution of Oceanography (SIO) and Harvard University, for the analysis of each of the more than 3,000 days of continuous GPS observations in the BIOFROST network.

The main characteristics of this software are that dual-frequency GPS observations from each day are analyzed using *GAMIT*. The results are computed loosely constrained Cartesian coordinates for stations, satellite orbit parameters, as well as their mutual dependencies. *GAMIT* results from analyzed sub-networks are then combined using *GLOBK*, where the reference frame is also realized. This procedure results in daily estimates of positions for all sites included in the analysis in a well-defined reference frame. Using *GLOBK*, it is possible to combine several days (and years) of GAMIT results and estimate initial site positions and velocities, and apply constraints for reference frame realization in one step. This last facility has however not been utilized in this study.

Primarily for practical reasons, we divided the BIFROST network into five sub-networks (Sweden, Finland, Norway, Denmark, and – as a "backbone" sub-network – the EPN stations), including some over-

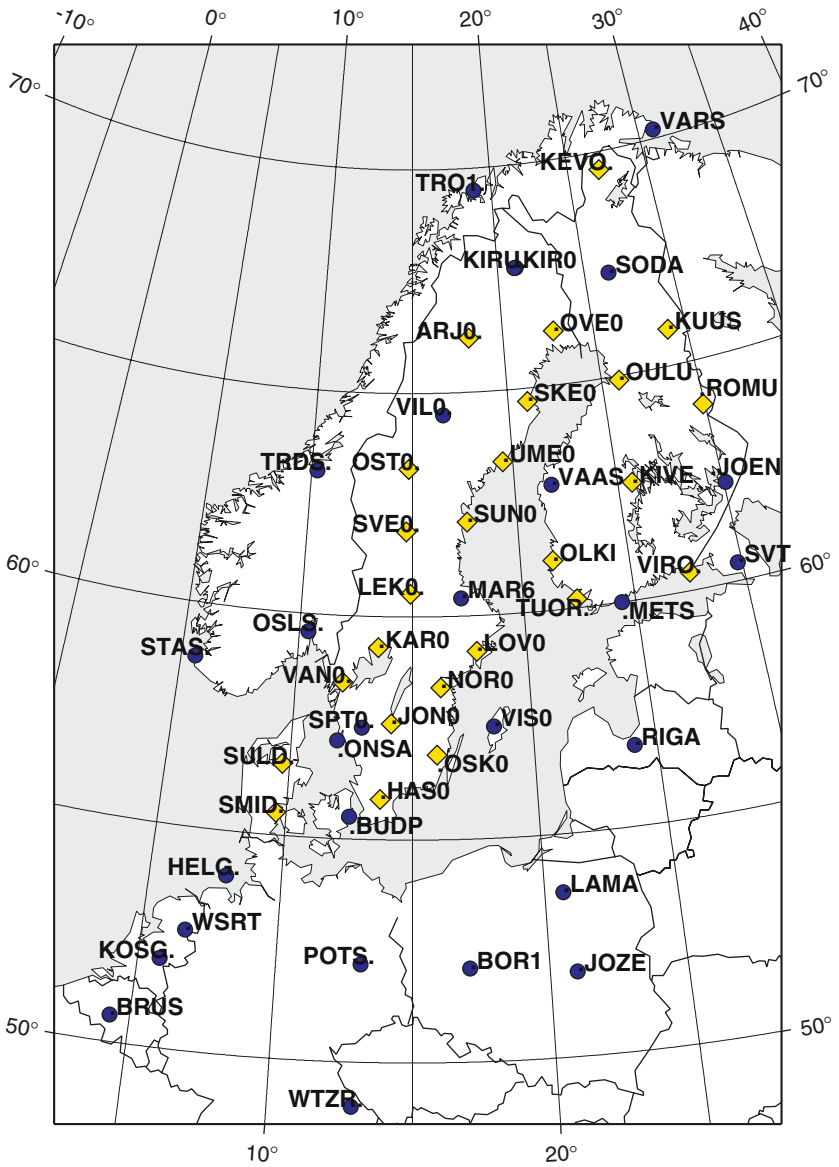

Fig. 1 Map showing the sites used in this study. Sites included in the EUREF Permanent Network (EPN) are marked with *dots*, while other BIFROST sites are marked with *diamonds*

lapping stations. For each network, double-differenced GPS carrier-phase and code pseudorange observations were analyzed in daily sessions using *GAMIT* with a 10° elevation cut-off angle, atmospheric zenith delays were estimated every 2 h (piecewise-linear model) together with daily gradient parameters, and the Niell (1996) mapping functions were used.

The carrier-phase observations were assigned elevation-angle-dependent weights determined individually for each station and day from a preliminary solution, and GPS carrier-phase ambiguities were estimated to integers as far as possible. For the elevation-angle-dependent (ε) weighting, the model $\sigma^2_{\text{phase}} = A^2 + B^2/\sin(\varepsilon)$ was used, where the parameters A and B were determined from the preliminary solution. Station motion associated with ocean tide loading (OTL) and solid Earth tides were modeled, and a priori orbits from the Scripps Orbit and Permanent Array Center (SOPAC), "g-files", were used. The output from *GAMIT* are the so-called quasi-observations including loosely constrained 3D Cartesian coordinates for each station, 18 orbit parameters for each satellite (of which 15 were estimated in the solution), and six Earth orientation parameters, including mutual dependencies.

In the second step of the processing, *GLOBK* was used for combining our regional sub-networks with global networks, computed by SOPAC, into single-day unconstrained solutions. Finally, constraints that represent the reference frame realization were applied by using a set of globally distributed fiducial stations and

solving for translations, rotations and a scale factor (seven-parameter Helmert model), as well as a slight adjustment of the satellite orbit parameters. The result comprises stabilized daily station positions, satellite orbit parameters, and Earth orientation parameters (EOPs) (cf. Nikolaidis 2002).

The measure to solve for a scale factor in the *GLOBK* step deserves some special attention. It may be argued that from a theoretical point of view, the scale in GPS is defined by the speed of light (c) and gravitational coefficient (GM), and therefore the scale factor should be consistent with zero (Tregoning and van Dam 2005, and the references therein). In earlier studies using *GAMIT/GLOBK*, the estimation of a scale factor has usually not been included in the stabilization step (e.g., McClusky et al. 2000). However, in, e.g., McClusky et al. (2000), the stabilization was done regionally and the primary interest of the study was velocities in the horizontal components, while the vertical was of minor interest to them.

For global analysis, Nikolaidis (2002) solved for a scale factor. Tregoning and van Dam (2005) showed [by simulation] that solving for a scale factor, when correction for atmospheric pressure loading (ATML) has not been applied (which is the case for our study), may introduce scale errors of up to 0.3 ppb and daily height errors up to 4 mm. Ge et al. (2005) found that biases in the GPS antenna phase centre offsets, e.g., by using the IGS standard values for Block-IIR GPS satellites, led to a scale change of more than 1 ppb.

In our study, we have used relative satellite and receiver antenna models, and not the recently available absolute antenna models. Therefore, we conclude that it is reasonable to solve for a scale factor, although it may introduce some aliasing effects due to the omitted ATML correction. Our choice not to trust the stability in the scale from the GPS analysis is further supported by Kedar et al. (2003), where it is showed that the corrections for the higher order ionospheric terms, which is commonly ignored in GPS analyses (only the first-order term is accounted for through the ionosphere-free linear combination; cf. Kim and Tinin 2006), effect the station positions at the 0.5-cm level in latitude and height.

In Fig. 2, the estimated daily scale factors from our study are plotted. The trend and scatter is fairy similar to what has been shown in other studies (e.g., Fig. 1 of Ge et al. 2005).

3.2 Reference frame considerations

In this study, GPS data analysis has been employed to derive a 3D velocity field of the deformation of the Earth's crust in Fennoscandia, which is dominated by an ongoing GIA process. In order to resolve the slow and small-scale deformation of the region, a terrestrial reference frame (TRF) consistent over the time-period of the analysis is needed. We also would like to achieve a velocity field that is as independent as possible of any disturbance occurring at a single station. The natural choice was therefore global adaptation of our analysis to the latest version of the International Terrestrial Reference Frame (ITRF), ITRF2000 (Altamimi et al. 2002).

Following the strategy discussed above, the TRF realization was performed by constraining a number of globally distributed "good" stations using their a priori ITRF2000 position and velocity values as well as their respective variance estimates. The following criteria for being a "good" fiducial station for stabilization have been used. First, the station should be a high-quality ITRF2000 site, which is considered to be fulfilled for stations included in Table 2 of Altamimi et al. (2002).

Second, there should be no major changes of station hardware. Especially, changes of antennas and radomes are of concern. Third, the station position time series should be "clean" (usually determined by visual inspection after a preliminary stabilization) with respect to

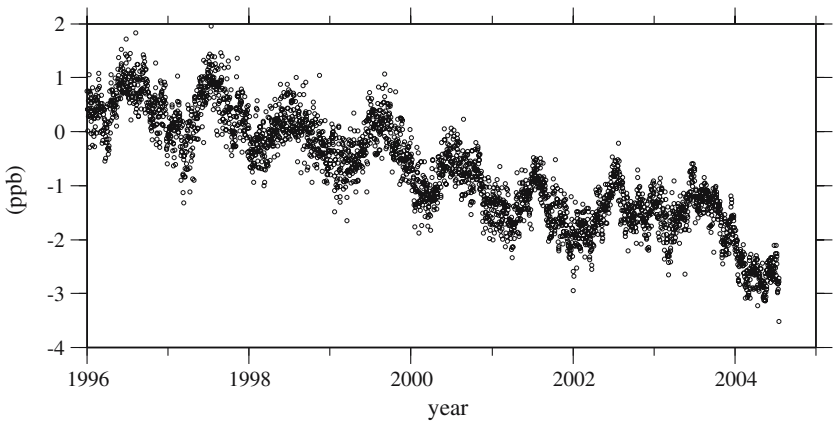

Fig. 2 Plot of estimated daily scale factors

jumps, large scatter, and unstable rate of motion. Fourth, sites located outside known deformation zones are preferred.

Because the selection of "stabilization" stations is a trade-off between having only stations that comply with the criteria above, and having a large number of fiducial stations with good global coverage, two different approaches have been utilized. In the first selection, we have used only stations on assumed rigid parts of tectonic plates that fulfil the criteria well. This leads to a selection of 21 fiducial stations (filled dots in Fig. 3).

In the second selection of 44 sites, we have been more moderate and also accepted stations within deforming zones. The two approaches result in a difference in north and east velocity of about 0.2 mm/year and a difference in vertical velocity of about 0.1 mm/year within our area of interest. Considering the formal velocity error in ITRF2000 of the selected "stabilizing" stations, which is usually a few times larger than these differences (cf. Altamimi et al. 2002), the two approaches (using the 21 or 44 "stabilization" site selection) may be considered equally good.

Accepting the idea that redundancy is better for a "stabilization" based on more sites, we have decided to present the velocity field based on the 44 stabilizing sites in the following analysis, and thereby reducing the influences from possible perturbations at individual stations.

The outcome of the process described above is daily GPS-derived position estimates for each station constrained to ITRF2000, where the evolution of the position estimates is dependent of the ITRF2000 velocity field globally. We should, therefore, be aware of possible contamination of our results due to shortcomings in the ITRF2000 reference frame. In principle, the scale in ITRF2000 is derived from observations using VLBI (Very Long Baseline Interferometry) and SLR/LLR (Satellite and Lunar Laser Ranging), while the geocenter is derived from SLR/LLR.

The same will therefore be valid also for possible changes in scale or stability of the geocenter in ITRF2000; e.g., an instability in the geocenter would map at a 1:1 ratio into derived station velocities, while a possible instability in scale at the 0.1 ppb/year could contaminate the derived vertical velocity by about 0.5 mm/year. This is most critical for the vertical component, while it is less important for the evaluation of horizontal velocities, where a transformation approach is usually applied (Sect. 5.3).

Although the reference frame issue is crucial for how useful the GPS-derived 3D velocity field will be, while comparing to other physical phenomena, such as sea-level variations, we concentrate on presentation of the new 3D motion field and leave a discussion on reference frame issues for a separate paper.

3.3 Time-series analysis and data editing

As mentioned above, it is possible to use *GLOBK* to estimate station velocities (provided that sufficient computer capacity is available). As such, this has not been

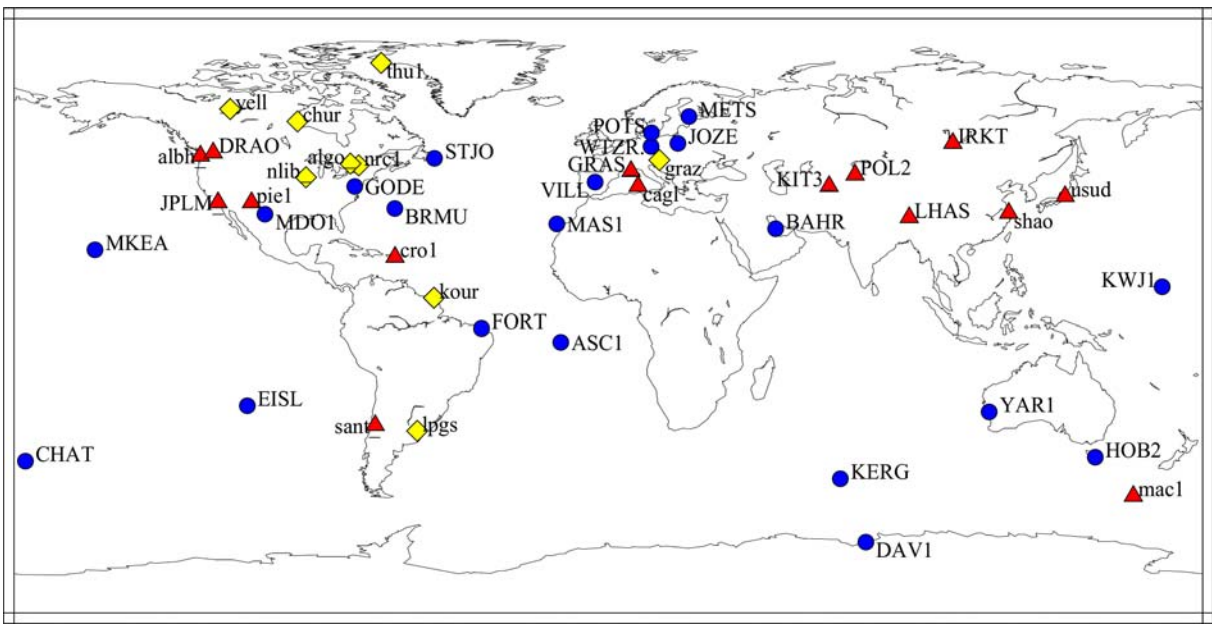

Fig. 3 Sites used for reference frame realization. *Dots* are the selection of 21 sites (see the text), *diamonds* are additional intra-plate sites, and *triangles* are sites located in deforming zones. Site identification in *lower case* indicates less well-determined time series

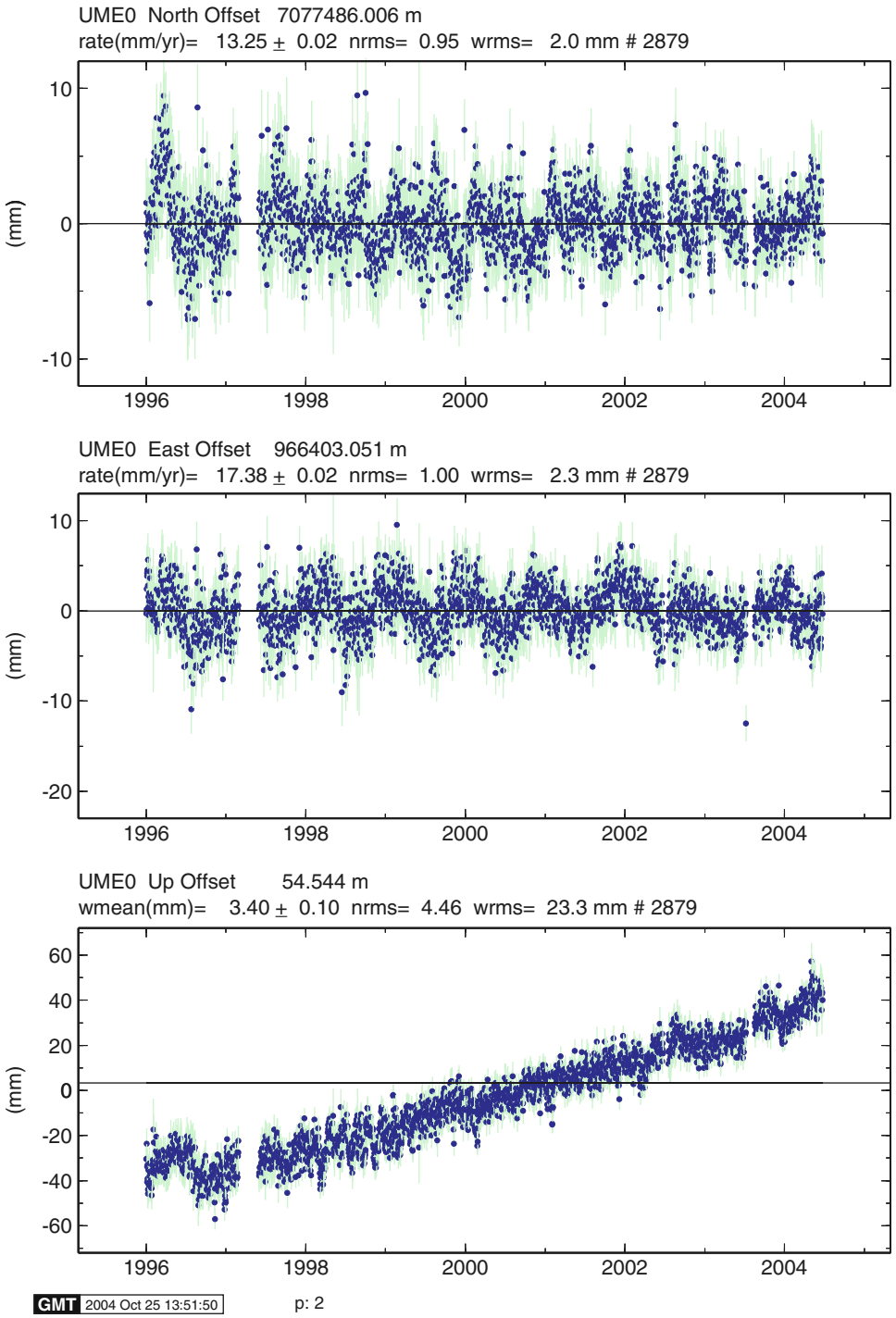

Fig. 4 Example from UME0 of position time series before editing. The vertical "jump" in August 1996 is due to removal of a radome of unsatisfactory design. Clear seasonal variations can also be seen, especially in the East direction

done here. Instead, we apply time-series analysis and data editing to obtain reliable velocity estimates together with their uncertainties for each station, based on their daily position estimates.

An example of position time series before editing from the UME0 and KIVE stations are found in Figs. 4 and 5, respectively. Note that the north and east components have been de-trended before plotting. In August 1996, a shift in the height component for UME0 can be seen (Fig. 4). This is due to removal of a radome of a less satisfactory design and manufacturing; see Johansson et al. (2002) for a detailed discussion on antenna radomes in the BIFROST network.

We also see seasonal variations, especially in the east component in this case (Figs. 4, 5). A detailed discussion on seasonal variations in GPS-derived position time series may be found in Dong et al. (2002). A specific study on aliased tidal signatures in GPS time series is

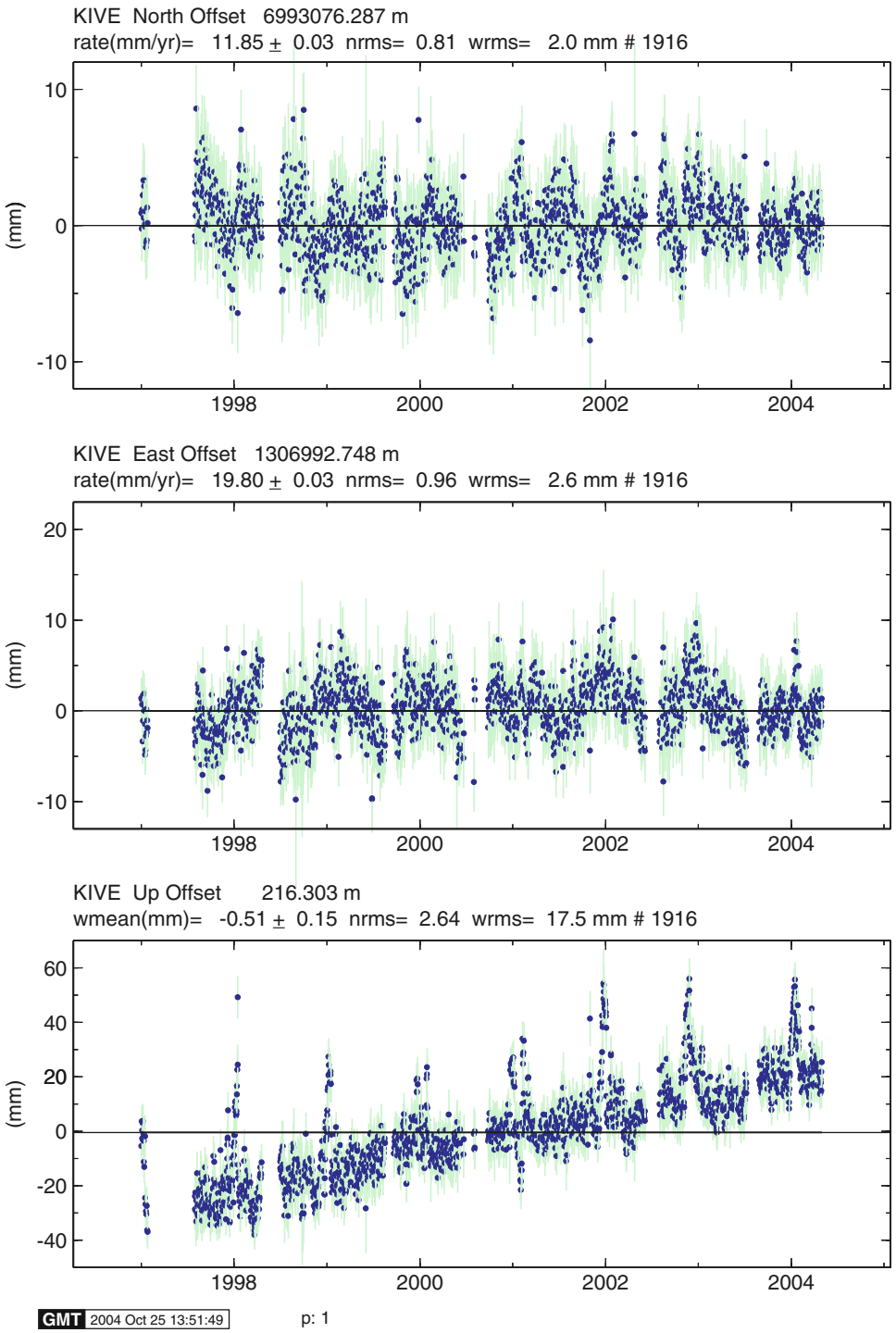

Fig. 5 Example from KIVE of position time series before editing. The outliers in the vertical component are considered to be caused by snow accumulation on the GPS antenna

presented in Penna and Stewart (2003), the propagation of unmodeled systematic errors into coordinate time series is investigated in Stewart et al. (2005), and periodic effects from different Earth tide models are presented in Watson et al. (2006).

From KIVE (Fig. 5), we also see groups of outliers, mainly in the vertical component. Since this phenomenon has shown to be more pronounced at northern inland sites, and during the northern winter season, it has been attributed to the accumulation of snow and ice on the radome or antenna (cf. Johansson et al. 2002). This accumulation will cause an additional propagation delay for the GPS signal.

In our GPS processing, we solve for atmospheric zenith delays in the neutral atmosphere, using a mapping function that maps an observed delay at a certain

elevation angle to zenith. Because the additional path delay caused by the accumulated snow or ice will not follow the elevation dependence exactly as expressed in our mapping function, the result will be an error in estimated vertical position.

We also notice occasional perturbations in the horizontal position estimates, which we relate to eccentric accumulation of snow on the antenna. Usually the outliers are positive in the vertical component (i.e., the estimated vertical position is too high), but may also be negative. This may depend on the shape of the accumulated snow and ice.

3.3.1 Model for estimating station velocities

Station velocities are estimated from daily estimates of the GPS station positions in ITRF2000 using an extended linear regression model. When estimating the constant velocity for each component of each station, we simultaneously model seasonal variations by estimating the amplitude of annual and semi-annual sine and cosine functions. The position shifts discussed above are modeled as a step function. Thus, six parameters plus one parameter for each shift are estimated for each component.

The mathematical expression for the model may be written as (e.g., Nikolaidis 2002):

$$\begin{aligned} y(t_i) = {} & a + bt_i + c\sin(2\pi t_i) + d\cos(2\pi t_i) \\ & + e\sin(4\pi t_i) + f\cos(4\pi t_i) \\ & + \sum_{j=1}^{n_g} g_j H(t_i - T_{gj}) + v_i, \end{aligned} \tag{1}$$

where t_i are epoch times in years for the daily solutions, H is the Heaviside step function, and v_i denotes noise.

3.3.2 Outlier editing

The purpose of outlier editing is to remove erroneous samples from disturbing the estimated station velocities. An additional purpose is to retrieve a "clean" data set that belongs to one stochastic distribution, where the residuals from the deterministic model (v_i above) can be used for estimating the precision of the derived parameters.

We have used the *Tsview* software [Herring 2003; MIT 2005, (*online*)] for data editing and estimation of station velocities. *Tsview* is a part of the *GGMatlab* tools that allows interactive viewing and manipulation of GPS velocities and time series with a *Matlab*-based graphical user interface.

For data editing, we have used an automatic outlier function in *Tsview* with a five-sigma rejection level. For northern sites with obvious snow problems, we have narrowed this to a three-sigma rejection level, occasionally supported by manual editing. Roughly some 30 data points per year have been removed using this method. Rejecting almost 10% of the data using the three-sigma level may be considered severe. However, the "snow" samples do not belong to the same stochastic distribution as the "clean" (no snow) samples. Thus, it could be argued that the percentage of rejected data points is somewhat irrelevant.

Other methods may be used for handling the snow problem: Kaniuth and Vetter (2004) estimate short-period local height biases. In Johansson et al. (2002), the "snow samples" have generally not been removed, but their effect has been reduced by the modeling of seasonal variation, where periodic terms with frequencies of one, two and three cycles per year were estimated. A third approach, used in Scherneck et al. (2002), is to remove all data from the northern winter season (November 1–March 31), which results in a loss of about 40% of the data points and eliminates the option to estimate seasonal variation parameters.

3.4 Accuracy estimates of the derived station velocities

Reliable accuracy estimates of our above-derived station velocities presuppose that the character of the noise of the position time series is known a priori, or that it can be estimated from the noise itself. Assuming a pure white noise model may result in underestimation of velocity errors by a factor of five or more (Mao et al. 1999). A common method to handle this problem is to determine the spectral index and amplitude of the noise using maximum likelihood estimation (MLE) (e.g., Williams 2003; Williams et al. 2004).

The "realistic sigma" function of *Tsview* used in this study takes a somewhat different approach. Formal uncertainties in derived parameters (assuming white noise) are scaled using a predicted Chi-squared-per degree of freedom, assuming a first-order Gauss–Markov process [MIT 2005 (online), Herring 2004-10-29, personal communication]. Weighted means and a weight for each mean are calculated for consecutive non-overlapping sub-segments of the residual time series, using sub-segments of a certain length. The next step is to calculate the Chi-squared-per degree of freedom for this sample of means. The process is repeated for longer and longer sub-segment lengths.

By studying the increase of the Chi-squared-per degree of freedom with increasing length of the sub-segments, the Chi-squared-per degree of freedom for infinitely long average sub-segments is predicted. The "realistic sigma" calculation results in an accuracy

Table 1 Computed velocity field and accuracy estimates (1σ), transformed using the ITRF2000 absolute rotation pole to Eurasia

Site name	Site abbrev	N_{vel} (mm/year)	E_{vel} (mm/year)	U_{vel} (mm/year)	N +/− (mm/year)	E +/− (mm/year)	U +/− (mm/year)	Length (year)
Arjeplog	ARJ0	0.68	−0.80	7.65	0.06	0.09	0.24	8.5
	BOR1	0.26	0.32	−0.74	0.06	0.18	0.24	8.5
	BRUS	−0.42	−0.34	0.83	0.16	0.11	0.25	8.5
	BUDP	−0.08	−0.43	−0.24	0.17	0.11	0.53	5.5
Hässleholm	HAS0	−0.04	−0.55	1.40	0.05	0.07	0.30	8.5
	HELG	0.55	−0.53	0.24	0.11	0.12	0.29	4.4
Joensu	JOEN	−0.72	0.51	4.06	0.08	0.09	0.19	7.5
Jönköping	JON0	−0.59	−0.41	2.83	0.07	0.05	0.22	8.3
	JOZE	0.24	0.16	0.72	0.07	0.12	0.18	8.5
Karlstad	KAR0	−0.10	−0.64	4.86	0.06	0.07	0.18	8.5
Kevo	KEVO	0.17	−0.01	3.53	0.07	0.11	0.26	7.3
Kiruna	KIR0	0.40	−0.48	6.36	0.07	0.14	0.28	8.3
	KIRU	0.54	−0.03	5.96	0.35	0.50	0.69	8.5
Kivetty	KIVE	−0.69	0.62	7.22	0.07	0.11	0.19	7.3
	KOSG	0.83	0.12	−1.02	0.08	0.08	0.25	8.5
Kuusamo	KUUS	−0.56	0.73	7.66	0.06	0.12	0.18	7.3
	LAMA	0.19	0.00	−0.99	0.19	0.18	0.46	8.5
Leksand	LEK0	−0.68	−0.40	7.75	0.24	0.09	0.19	8.5
Lovö	LOV0	−0.59	−0.08	5.64	0.04	0.09	0.16	8.5
Mårtsbo	MAR6	−0.54	−0.22	6.74	0.05	0.09	0.15	8.3
Metsähovi	METS	−0.87	0.53	4.26	0.04	0.06	0.23	8.5
Norrköping	NOR0	−0.53	−0.17	4.93	0.05	0.06	0.20	8.5
Olkiluoto	OLKI	−0.74	0.33	7.26	0.05	0.08	0.20	7.3
Onsala	ONSA	−0.52	−0.70	2.66	0.13	0.09	0.31	8.3
Oskarshamn	OSK0	−0.35	−0.25	2.88	0.05	0.09	0.19	8.5
	OSLS	0.11	−1.04	5.78	0.16	0.17	0.42	5.3
Östersund	OST0	0.43	−1.02	8.26	0.04	0.07	0.17	8.5
Oulu	OULU	−0.29	0.56	8.82	0.06	0.11	0.21	7.3
Överkalix	OVE0	0.02	0.11	8.80	0.07	0.11	0.21	8.5
	POTS	0.08	−0.29	−0.56	0.05	0.06	0.29	8.5
Riga	RIGA	−0.26	−0.01	1.81	0.06	0.10	0.25	8.2
Romuvaara	ROMU	−0.69	0.74	5.84	0.06	0.09	0.17	7.3
Skellefteå	SKE0	0.40	−0.38	9.61	0.08	0.08	0.18	8.3
	SMID	−0.60	−1.33	0.86	0.26	0.20	0.73	4.2
Sodankylä	SODA	0.15	0.25	7.12	0.11	0.17	0.31	7.4
Borås	SPT0	−0.37	−0.80	3.48	0.04	0.06	0.25	8.0
	STAS	0.24	−1.06	1.18	0.10	0.15	0.51	5.3
	SULD	−0.27	−0.55	0.62	0.11	0.13	0.47	4.2
Sundsvall	SUN0	−0.14	−0.35	9.24	0.05	0.09	0.18	8.5
Sveg	SVE0	0.30	−0.82	7.54	0.05	0.07	0.21	8.5
	SVTL	−1.04	0.54	2.53	0.10	0.09	0.27	8.2
	TRDS	0.88	−1.82	3.80	0.11	0.14	0.58	5.3
	TRO1	2.11	0.35	2.30	0.28	0.39	0.49	6.4
Tromsö	TROM							
Tuorla	TUOR	−0.69	0.15	5.83	0.08	0.06	0.20	7.3
Umeå	UME0	−0.13	−0.26	10.06	0.06	0.08	0.17	8.5
Vaasa	VAAS	−0.51	0.23	8.62	0.05	0.08	0.19	7.5
Vänersborg	VAN0	−0.03	−0.97	4.10	0.05	0.08	0.17	8.3
	VARS	−0.43	−0.48	1.89	0.11	0.17	1.13	5.3
Vilhelmina	VIL0	0.35	−0.88	8.39	0.06	0.12	0.16	8.3
Virolahti	VIRO	−0.81	0.22	3.48	0.06	0.10	0.21	7.3
Visby	VIS0	−0.47	−0.05	3.10	0.04	0.13	0.17	8.3
	WSRT	0.95	−0.44	−0.23	0.07	0.13	0.34	7.1
	WTZR	0.42	0.10	0.05	0.07	0.05	0.27	8.5

Site names are those used in Johansson et al. (2002), and site abbreviations are those used by the IGS, EPN or national geodetic authorities. Length is difference in years between first and last observation in the position time series

estimate that is usually about 2–6 times larger compared to accuracy estimates based on the white noise model. This is fairly well in agreement with findings in other studies (e.g., Scherneck et al. 2002), but somewhat low compared to, e.g., Mao et al. (1999). The noise properties of BIFROST GPS time series are also investigated using a fractal model in Bergstrand et al. (2006).

4 Results

The result from the process above is a 3D velocity field of the included stations constrained to the ITRF2000 velocity field. A major purpose behind this work, however, is management of geodetic reference frames within the area influenced by the GIA process. Therefore, our choice is to present the results in relation to the stable part of the Eurasian tectonic plate. The computed velocity field is thus transformed (rotated) using the ITRF2000 No-Net-Rotation (NNR) Absolute Rotation Pole for Eurasia in accordance with Table 1 of Altamimi et al. (2003). The result is presented in Table 1.

5 Analysis

5.1 Evaluation of the reference frame realization

In order to check our results, we first take a look at the velocities at sites where we initially would assume the effect from the GIA process is small. In Table 2, the mean, standard deviation and root-mean-square (RMS) value of the north and east velocities for the eight sites BOR1, BRUS, JOZE, KOSG, LAMA, POTS, RIGA and WTZR have been computed. The mean value of about 0.2 mm/year, is in the range of the differences between using 21 or 44 stabilization sites (see Sect. 3.2).

This indicates a successful reference frame realization without any serious bias, and is well within the formal error of the absolute Euler pole for Eurasia in ITRF2000 (0.02 mas/year or 0.6 mm/year; Altamimi et al. 2003). The standard deviation and RMS values also indicate an external accuracy for these eight relatively "good" stations at the 0.5 mm/year level, which however is a few times larger than the accuracy estimates in Table 1.

Table 2 Statistics of horizontal velocities of the permanent GPS stations BOR1 BRUS JOZE KOSG LAMA POTS RIGA and WTZR

	N_{vel} (mm/year)	E_{vel} (mm/year)
Mean	0.17	0.01
Standard deviation	0.39	0.22
RMS	0.40	0.21

5.2 Evaluation of vertical velocities

In Fig. 6 (shown later), the vertical velocities from this study are compared to the results from the BIFROST standard solution, to a model, and to land uplift values based on classical geodetic methods. The BIFROST standard solution presented in Johansson et al. (2002) is the current "official" BIFROST solution. It is based on observations between August 1993 and May 2000 from the permanent GPS networks of Finland and Sweden, supplemented by some additional IGS stations.

Johansson et al. (2002) analyzed the GPS data using the *GIPSY-OASIS II* software developed at the Jet Propulsion Laboratory (JPL) (e.g., Webb and Zumberge 1993). *GIPSY* is principally different from *GAMIT* in that it solves for all parameters (satellite and receiver clock parameters, etc.), rather than reducing their influence on estimated station positions by differencing techniques. This approach has developed towards the well-known precise point positioning (PPP) technique commonly applied together with *GIPSY* (Zumberge et al. 1997).

The BIFROST standard solution, however, is computed in a network approach utilizing a no-fiducial approach, where a priori station coordinates have weak constraints. A minimum elevation angle of 15° was adopted, atmospheric zenith delay parameters (but no gradients) were estimated, satellite orbits were highly constrained to the values distributed by the IGS, and corrections for motion associated with OTL and solid Earth tides were incorporated in the model. We note that the BIFROST standard solution comprises a period of intensive hardware modifications at the GPS stations in the BIFROST network, producing several shifts in the position time series that had to be accounted for.

In Table 3, we have also compared our results with the "winter edited" version of the BIFROST solution, hereafter called the WE solution, presented in Scherneck et al. (2002) (see Sect. 3.3.2).

Our result was also compared with the model computations presented in Milne et al. (2001). We use the particular model resolved as best fitting the BIFROST standard solution (Johansson et al. 2002). This model is the Fennoscandian ice load history of Lambeck et al. (1998a,b), a 120-km-thick lithosphere, an upper mantle viscosity of 8×10^{20} Pa s, and a lower mantle viscosity of 1×10^{22} Pa s.

Finally, we compare our results with the vertical velocities presented in Ekman (1998). These are based on apparent land uplift of the crust relative to local sea

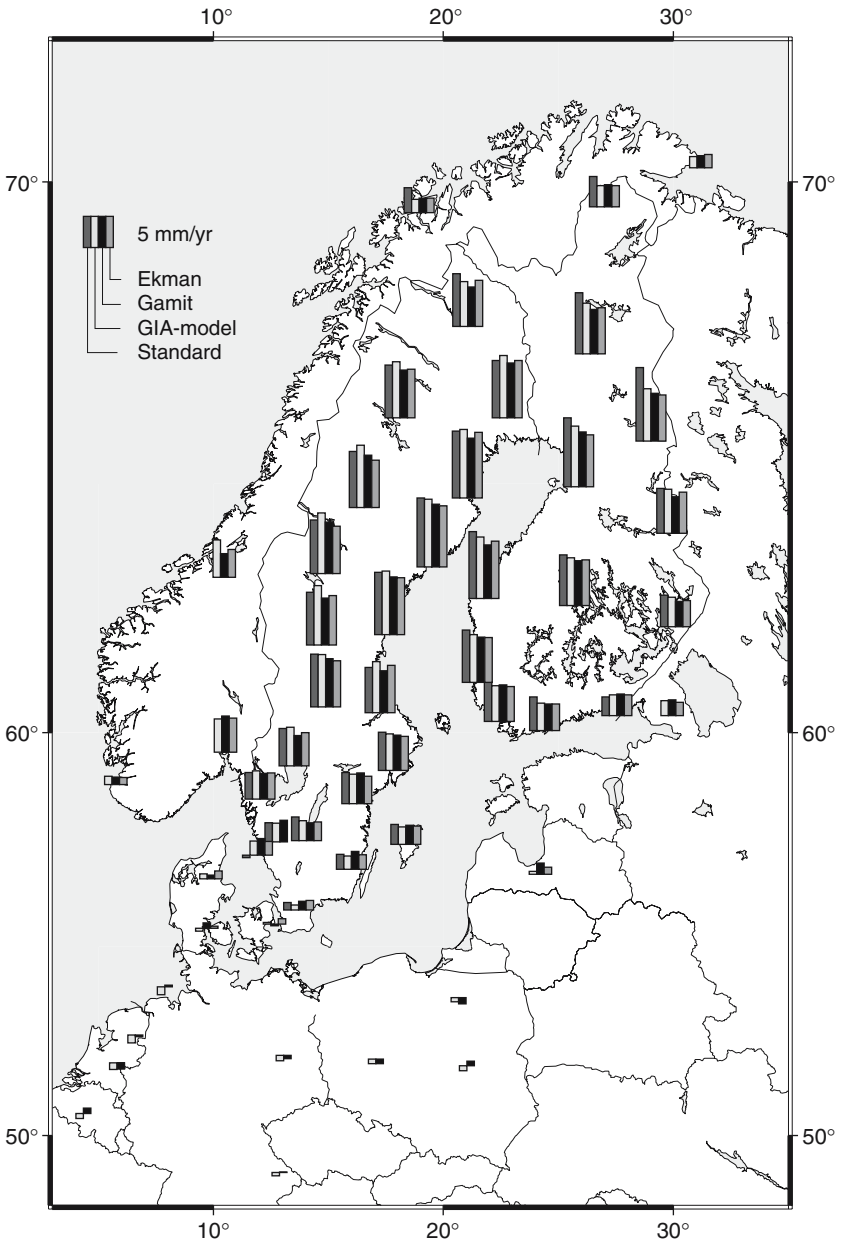

Fig. 6 Vertical rates from the current GPS solutions together with vertical rates from the standard solution, the GIA model, and the values from Ekman (1998) (see the text)

level observed at tide gauges during the 100-year period 1892–1991 as presented in Ekman (1996), where the inland is densified by repeated geodetic leveling, an eustatic sea-level rise of 1.2 mm/year has been applied, and the rise of the geoid (relative to the ellipsoid) is based on computations presented in Ekman and Mäkinen (1996). From a thorough discussion on the reliability (Ekman and Mäkinen 1996), the standard errors are estimated to between 0.3 and 0.5 mm/year, where the larger values apply to inland stations or stations with a weak connection (from repeated leveling) to the nearest tide gauge.

Comparing the BIFROST standard solution to our current solution, we get a bias (mean of differences; standard solution minus GAMIT solution) of 0.8 mm/year and a standard deviation of 1.2 mm/year. These values include northern inland stations from Finland, which have a shorter observation period in the standard solution (typically 3.5 years), and where the snow accumulation phenomenon has been the most pronounced. A second comparison, where only sites from Sweden are included, gives a bias and standard deviation between the standard and GAMIT solutions of 0.4 and 1.0 mm/year, respectively.

Comparing the WE solution and the GIA model to the current solution, we get a bias (mean of differences) of 0.5 and 0.3 mm/year, respectively. The computed standard deviation of differences is close to 1.0 mm/year for the WE solution and slightly lower for the GIA model, at

Table 3 Comparison of vertical rates between the standard solution (Johansson et al. 2002), "winter edited" (WE) version of the previous BIFROST solution (Scherneck et al. 2002), the GIA model from Milne et al. (2001), this new solution computed with *GAMIT/GLOBK*, and the vertical rate values computed by Ekman (1998) (see the text)

Site	Standard solution (mm/year)	WE solution (mm/year)	GIA model (mm/year)	GAMIT (mm/year)	Ekman (mm/year)
ARJ0	8.5	8.41	8.99	7.65	7.8
BOR1		–	−0.76	−0.74	–
BRUS		−2.10	−0.78	0.83	–
BUDP		–	0.24	−0.24	0.9
HAS0	1.2	1.39	0.78	1.40	1.5
HELG		–	−1.28	0.24	–
JOEN	5.1	5.49	4.75	4.06	4.2
JON0	3.8	4.01	3.21	2.83	3.0
JOZE		–	−0.77	0.72	–
KAR0	6.0	6.06	6.18	4.86	5.3
KEVO	4.9	4.60	3.40	3.53	3.4
KIR0	8.5	7.11	7.17	6.36	7.4
KIRU		6.98	7.19	5.96	7.4
KIVE	8.1	7.94	7.67	7.22	7.3
KOSG		−1.10	−1.09	−1.02	–
KUUS	11.8	8.09	8.40	7.66	7.4
LAMA		–	−0.66	−0.99	–
LEK0	8.5	8.66	8.38	7.75	7.4
LOV0	6.1	6.24	5.89	5.64	5.5
MAR6	7.3	7.03	8.21	6.74	7.6
METS	5.4	5.57	4.39	4.26	4.3
NOR0	5.0	5.22	4.76	4.93	4.4
OLKI	8.4	7.82	7.67	7.26	7.2
ONSA	−0.4	0.46	2.26	2.66	2.2
OSK0	2.4	2.39	2.16	2.88	2.3
OSLS		–	5.34	5.78	5.5
OST0	8.6	8.26	9.72	8.26	7.6
OULU	11.1	10.46	9.71	8.82	8.3
OVE0	9.2	8.85	10.03	8.80	9.2
POTS		−1.54	−0.84	−0.56	–
RIGA		2.54	0.45	1.81	1.1
ROMU	7.2	7.25	7.10	5.84	6.6
SKE0	10.7	10.98	11.01	9.61	10.5
SMID		–	−0.45	0.86	0.3
SODA	9.8	9.50	8.13	7.12	7.4
SPT0	3.1	2.85	2.99	3.48	–
STAS		–	1.31	1.18	1.1
SULD		–	0.80	0.62	1.3
SUN0	10.0	10.22	10.19	9.24	9.1
SVE0	8.5	8.31	9.52	7.54	7.9
SVTL		–	2.42	2.53	2.1
TRDS		–	5.99	3.80	4.5
TRO1			2.17	2.30	2.3
TROM	4.0	3.10	2.17	2.30	2.3
TUOR	6.3	6.45	5.75	5.83	5.6
UME0	11.1	11.00	10.89	10.06	9.8
VAAS	10.7	10.26	9.88	8.62	9.2
VAN0	4.3	4.42	4.50	4.10	4.2
VARS		–	1.80	1.89	2.1
VIL0	9.0	8.40	9.99	8.39	7.6
VIRO	3.0	3.72	3.36	3.48	3.3
VIS0	3.2	3.60	2.79	3.10	2.9
WSRT		–	−1.24	−0.23	–
WTZR		−0.44	−0.53	0.05	–

0.9 mm/year. The comparison to the values from Ekman (1998) gives a bias of 0.1 mm/year and standard deviation of 0.5 mm/year. Avoiding the (according to Ekman 1998) less reliable inland stations in the analysis gives a bias close to zero, and a slightly reduced standard deviation of 0.4 mm/year. A summary of the comparison is given in Table 4.

The comparison (Table 4) shows a very good consistency between the presented solution and land uplift values derived from classical geodetic methods. The scatter clearly shows that we are able to determine vertical velocities for our permanent GPS stations at the 0.5-mm/year level. In the comparison to the previous BIFROST solutions and the GIA model, the values for the vertical velocities of the current solution are consistently lower at the 0.5-mm/year level. However, at the area for maximum land uplift (ARJ0, OVE0, OULU, SKE0, SUN0, UME0, VAAS, VIL0; cf. Fig. 1) the values from the model are at the 1 mm/year higher than the presented solution.

While the used GIA model has been tuned to the previous BIFROST velocities (see earlier), an overestimated ice thickness and glaciation period in the central parts, as well as shortcomings of the previous BIFROST solution, used for determination of GIA parameters (here; lithosphere thickness, upper and lower mantle viscosity) may contribute to the explanation.

From Fig. 6, we may also note that for the northernmost stations (TRO1, KEVO, VARS) vertical rates from the current solution, the GIA model and the values from Ekman (1998) all agree within 0.3 mm/year. Considering the less reliable velocity estimates at TRO1 and VARS shown as an increased standard error, which partly is due to unexplained irregularities in the position time series, some caution should be applied in the interpretation of the good agreement.

Considering the differences between the standard solution and the GAMIT solution, we recall the discussion in Sect. 3.2 on reference frames. The GAMIT solution is tuned to ITRF2000, while the standard solution relies on a reference frame derived from the GPS analysis performed at the JPL available at that time (northern spring 2000) (Johansson et al. 2002). An apparent bias between the two solutions at the 0.5 mm/year level is therefore within the expected uncertainty.

The same is valid for the WE solution, where the difference from the standard solution is primarily in the editing approach, while the reference frame handling is similar (Scherneck et al. 2002). However, the implication of this is that some care should be considered in using our results in other applications. For example, for sea-level work, where the absolute sea-level rise is estimated from apparent sea-level rise observed at tide gauges minus absolute vertical rate observed by GPS (and a correction for the change of the geoid), the uncertainty in the geodetic reference frame may be one of the major contributors to the error budget.

While comparing the standard solution and the GAMIT solution we also note that a different elevation cut-off angle has been used in the GPS analysis (15° and 10°, respectively), which also may influence the derived velocity values. This problem will be addressed further in a forthcoming paper.

Recently, we became aware that the IERS92 Earth tide model was implemented in *GAMIT* version 10.1 and hence used in this study. This model may cause systematic errors in derived vertical station velocities at the 0.1-mm/year level compared to the more recent IERS2003 model (Watson et al. 2006). This possible error source should therefore be added to the error budget of the presented station velocities (Table 1).

5.3 Evaluation of horizontal velocities

From the evaluation of the reference frame realization, we got a first indication of the reliability of the presented velocity field.

Here, we compare our solution to the same GIA model of Milne et al. (2001). When we compare horizontal velocity components and GIA models, we ad-

Table 4 Statistics from the comparison of vertical rates from the standard solution, the WE solution, the GIA model and values from Ekman relative to the *GAMIT* solution (this paper)

Difference to GAMIT solution (mm/year)	Mean	Standard deviation
BIFROST standard	0.8	1.2
BIFROST standard (Swedish sites only)	0.4	1.0
WE solution	0.5	1.0
GIA model from Milne	0.3	0.9
Ekman	0.1	0.5
Ekman, "best stations"	0.0	0.4

The comparison is done by "standard", "WE", etc., minus the *GAMIT* solution

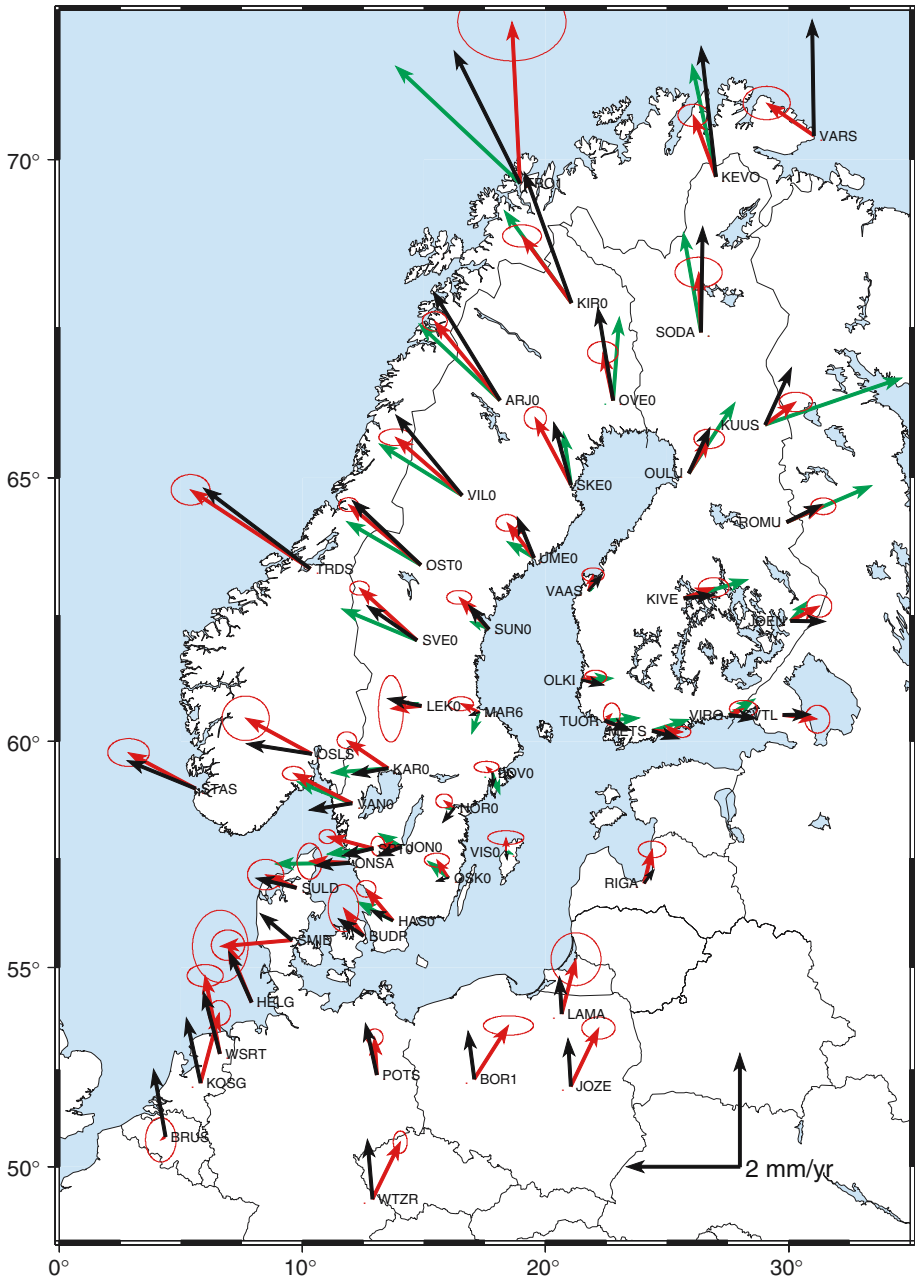

Fig. 7 The velocity field of the current solution rotated to fit the GIA model as described above, the velocity field from the standard solution (Johansson et al. 2002) rotated likewise, and the velocity field of the GIA model. *Arrows* for the model is in *black*, the standard solution in *gray*, and the new GAMIT solution *dark gray*, all with 95% probability *ellipses*

just a rigid rotation. The reason is that (a) the GIA model contains a global net rotation (a polar motion component) due to contemporary mass redistribution and loading in the global ocean (Milne and Mitrovica 1998); (b) the GIA model produces far-field motion due to the Laurentide ice sheet, which is rather uniform in the Fennoscandian region, i.e., to a large part indistinguishable from a rigid rotation of the Fennoscandian network; and (c) the net motion of the global geodetic stations in the ITRF2000 are constrained to the no-net rotation condition of NUVEL-1a-NNR. As the latter model is incomplete with respect to global motion (like additional, unaccounted-for terms associated with secular polar motion), and since such components cannot uniquely be resolved, we have to allow for this degree of freedom.

Using all 53 stations in the adjustment results in a standard deviation of 0.5 mm/year. Six of the sites deviate by more than 1 mm/year (BRUS, KIR0, KIRU, KEVO, TRO1 and VARS). The large deviation at the most northern sites may indicate some possibilities for improvements in the model in this region.

In Fig. 7, the velocity field of the current solution rotated as described above, the velocity field from the

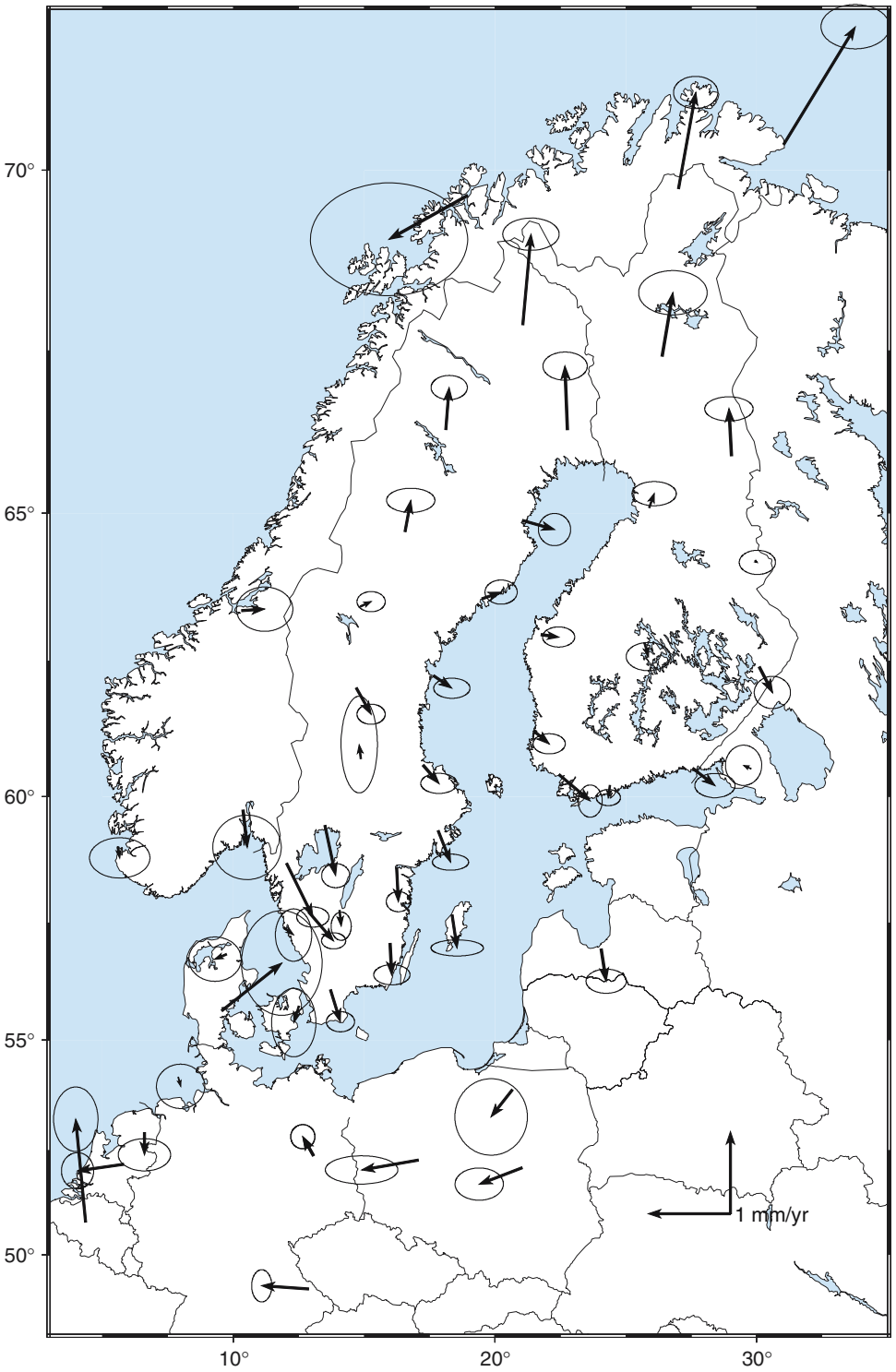

Fig. 8 Horizontal velocity differences of the GIA model minus GPS estimates (current GAMIT solution), after rotation to minimize differences from the GIA model

standard solution rotated likewise, and the velocity field of the GIA model is displayed.

The measure taken to rotate our velocity field to best fit the GIA model, while comparing the horizontal components of the GPS-derived velocity field, may be criticized, as follows. To add a second rotation pole to model intra-plate deformations would disturb the concept of NNR, which is the basis for conserving angular momentum of the Earth. This step was however done to compare the internal shape of two GPS-derived velocity fields to the model velocity field. For future applications where intra-plate deformations due to GIA must be taken into account in transformations for geodetic surveying applications, the most likely approach will be

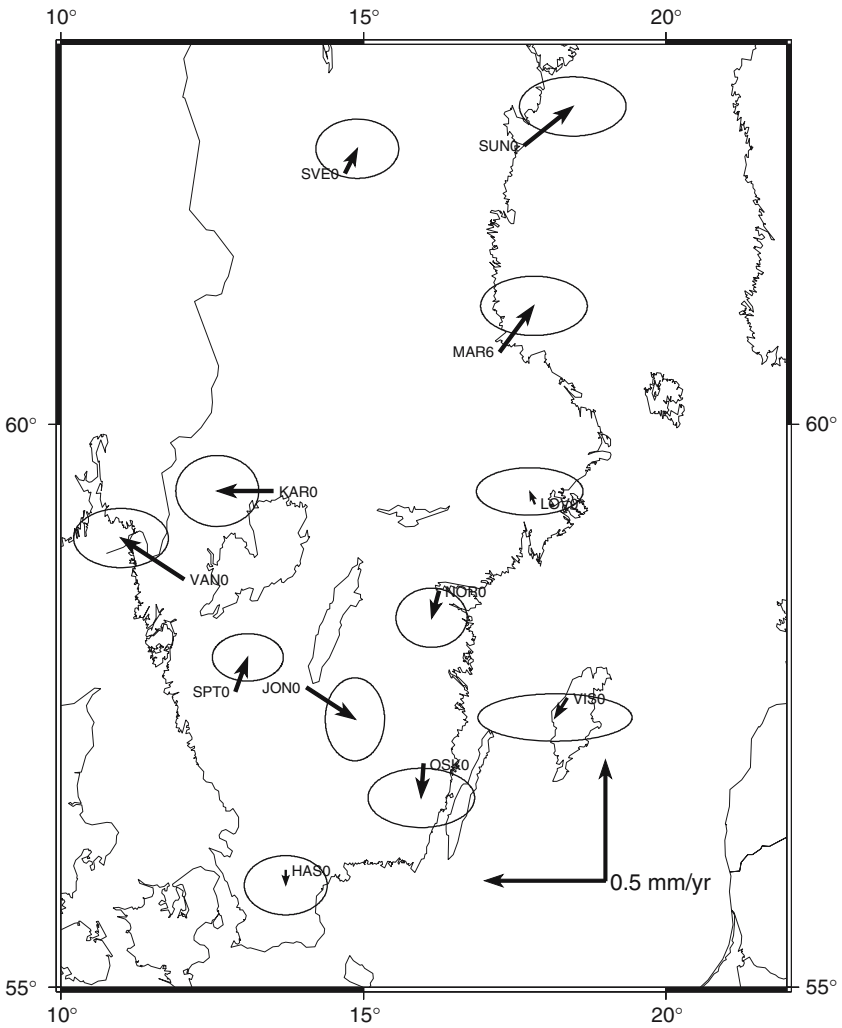

Fig. 9 Residuals in horizontal velocity after rotation of the current *GAMIT* solution to best fit the GIA model at the 12 stations in southern Sweden. The stations ONSA and LEK0 have been excluded due to changes of antennas or antenna radomes within the period of our study

to transform (rotate) the GIA model to the Eurasia rotation vector.

In Fig. 8, we have compared horizontal velocities from the GIA model (which is tuned to the previous BIFROST solution) to our GPS solution (here) after the rotations as described above. We note good agreement in central Fennoscandia, while the GIA model in the north shows overestimated horizontal velocities away from maximum land uplift area. This tendency is also visible in southern Sweden. Comparing this with the discussion on the differences in the vertical component (Sect. 5.2), we may conclude that the GIA model predicts slightly larger station rates in horizontal as well as vertical component compared to the current GPS solution.

The accuracy estimates above may be biased by possible shortcomings in some parts of the model and less accurate velocity estimates at GPS sites with shorter observation spans. To get a better assessment of the true scatter in the horizontal components of our presented GPS-derived velocities, we have performed a second transformation (rotation) using only 12 well-behaving stations in the southern part of Sweden, where the GIA model is assumed to perform best. The obtained RMS values of the residuals after the rotation are 0.14 and 0.11 mm/year for the north and east components, respectively. The residuals are displayed in Fig. 9.

6 Conclusions

We have derived a 3D velocity field for permanent GPS stations in the area subjected to the Fennoscandian glacial isostatic adjustment (GIA) process, based on continuous GPS observations between January 1996 and June 2004. Our approach for reference frame realization has demonstrated global adaptation to the ITRF2000 velocity field at the sub-mm/year level. The external assessment of the derived velocity field indicates an accuracy in the vertical component at the 0.5 mm/year (1σ), and

an internal consistency of 0.2 mm/year (1σ) for the horizontal component for the best GPS stations with long observation spans.

However, from a short review of geodetic reference frames, we conclude that some care should be considered if using the results from this study for other interpretations such as sea-level work. We also note that for future work, the forthcoming ITRF2005 may reduce some limitations in the currently available geodetic reference frames.

These new results confirm earlier findings of maximum discrepancies between GIA models and observations in the north of Fennoscandia. The reason may be related to overestimated ice thickness and glaciation period in this region. In general, the new solutions are more coherent in the velocity field as some of the perturbations could be avoided.

Acknowledgements We thank those who operate permanent GPS stations and make their data available for this kind of study. We are grateful to SOPAC for making quasi observations from global networks public available; MIT for the *GAMIT/GLOBK* software, and Glenn Milne for providing us with station velocities from the GIA model. The maps in this paper were generated using the generic mapping tools (GMT) (Wessel and Smith 1998). The US portion of this project was funded by the NASA Dynamics of the Solid Earth (DOSE) and Solid Earth and Natural Hazards (SENH) programs, and we thank the Swedish Science Foundation for the BIFROST support (G5103-20006292/2000). This particular study has been made possible thanks to support from Lantmäteriet (the National Land Survey of Sweden). Paul Tregoning and Simon Williams are thanked for their constructive reviews of this manuscript.

References

Altamimi Z, Sillard P, Boucher C (2002) ITRF 2000: a new release of the international terrestrial reference frame for earth science applications. J Geophys Res 107(B10):2214. DOI 10.1029/2001JB000561

Altamimi Z, Sillard P, Boucher C (2003) The impact of a no-net-rotation condition on ITRF2000. Geophys Res Lett 30(2):1064. DOI 10.1029/2002GL016279

Bergstrand S, Scherneck H-G, Lidberg M, Johansson J M (2006) BIFROST: noise properties of GPS time series. IAG/IAPSO/IABO joint assembly proceedings, Cairns, Springer (in press)

Dong D, Fang P, Bock Y, Cheng MK, Miyazaki S (2002) Anatomy of apparent seasonal variations from GPS-derived site position time series. J Geophys Res 107(B4). DOI 10.1029/2001JB000573

Ekman M (1991) A concise history of post glacial land uplift research (from its beginning to 1950). Terra Nova 3:358–365

Ekman M (1996) A consistent map of the postglacial uplift of Fennoscandia. Terra Nova 8:158–165

Ekman M (1998) Postglacial uplift rates for reducing vertical positions in geodetic reference systems. In: Jonsson B (ed) Proceedings of the General Assembly of the Nordic Geodetic Commission, May 25–29, ISSN 0280-5731 LMV-rapport 1999.12

Ekman M, Mäkinen J (1996) Recent postglacial rebound, gravity change and mantle flow in Fennoscandia. Geophys J Int 126:229–234

EUREF (2005) EUREF Permanent Network. http://www.epncb.oma.be/. Cited June 2005

FGI (2005) The Finnish Permanent GPS Network (FinnRef). http://www.fgi.fi/osastot/geodesia/projektit/finnref/index_eng.html. Cited June 2005

Ge M, Gendt G, Dick G, Zhang FP, Reigber C (2005) Impact of GPS satellite antenna offsets on scale changes in global network solutions. Geophys Res Lett 32 L06310. DOI 10.1029/2004GL022224

Herring T (2003) MATLAB Tools for viewing GPS velocities and time series. GPS solut 7:194–199

Frängsmyr T (1976) Upptäckten av istiden: studier i den moderna geologins framväxt = the discovery of the ice age. Almqvist & Wiksell, ISBN: 91-85286-08-7; ISBN: 91-85286-07-9

Johansson J M, Davis JL, Scherneck H-G, Milne GA, Vermeer M, Mitrovica JX, Bennett RA, Jonsson B, Elgered G, Elósegui P, Koivula H, Poutanen M, Rönnäng BO, Shapiro II (2002) Continuous GPS measurements of postglacial adjustment in Fennoscandia 1. Geodetic results. J Geophys Res 1079(B8). DOI 10.1029/2001B000400

Kaniuth K, Vetter S (2004) GPS estimates of postglacial uplift in Fennoscandia. Zeitchrift für Geodäsie. Geoinform Landmanage 129:168–175

Kedar S, Hajj G A, Wilson B D, Heflin M B (2003) The effect of the second order GPS ionospheric correction on receiver positions. Geophys Res Lett 30(16):1829. DOI 10.1029/2003GL017639

King RW (2002) Documentation for the GAMIT GPS analysis software. MIT Internal Report, 206 pp (http://www-gpsg.mit.edu/~simon/gtgk/GAMIT.pdf)

King RW, Herring TA (2002) Global Kalman filter VLBI and GPS analysis program, MIT Internal Report, 98 pp (http://www-gpsg.mit.edu/~simon/gtgk/GLOBK.pdf)

Kim BC, Tinin MV (2006) Contribution of Ionospheric Irregularities to the Error of Dual-frequency GNSS Positioning. J Geod (in press)

Koivula H, Ollikainen M, Poutanen M (1998) Use of the Finnish permanent GPS network (FinnNet) in regional GPS campaigns. In: Brunner FK (ed) Advances in positioning and reference frames. Springer, Berlin Hidelberg New York, pp 137–142

Lambeck K, Smither C, Johnston P (1998a) Sea-level change, glacial rebound, and mantle viscosity for northern Europe. Geophys J Int 134:102–144

Lambeck K, Smither C, Ekman M (1998b) Tests of glacial rebound models for Fennoscandinavia based on instrumented sea- and lake-lever records. Geophys J Int 135:375–387

Mao A, Harrison CGA, Dixon TH (1999) Noise in GPS coordinate time series. J Geophys Res 104:2797–2816

McClusky S, Balassanian S, Barka A, Demir C, Ergintav S, Georgiev I, Gurkan O, Hamburger M, Hurst K, Kahle H, Kastens K, Kekelidze G, King R, Kotzev V, Lenk O, Mahmoud S, Mishin A, Nadariya M, Ouzounis A, Paraadissis D, Peter Y, Prilepin M, Reilinger R, Sanli I, Seeger H, Tealeb A, Toksöz M N, Veis G (2000) Global positioning system constraints on plate kinematics and dynamics in the eastern Mediterrainan and Caucasus. J Geophys Res 1059(B3):5695–5719 (1999JB900351)

Milne GA, Mitrovica JX (1998) Postglacial sea-level change on a rotating earth. Geophys J Int 133(1):1–19

Milne GA, Davis JL, Mitrovica JX, Scherneck H-G, Johansson JM, Vermeer M, Koivula H (2001) Space-geodetic constraints on glacial isostatic adjustments in fennoscandia. Science 291:2381–2385

MIT (2005) GAMIT/GLOBK Matlab Tools. http://geoweb.mit.edu/~tah/GGMatlab/. Cited June 2005

Niell AE (1996) Global mapping functions for the atmosphere delay at radio wavelengths. J Geophys Res 101:3228–3246

Nikolaidis RM (2002) Observation of geodetic and seismic deformation with the global positioning system. Ph.D. thesis, University of California, San Diego

Panafidina N, Malkin Z, Webber R (2006) A new combined European Permanent Network station coordinates solution. J Geod (in press)

Penna NT, Stewart MP (2003) Aliased tidal signatures in continuous GPS height time series. Geophys Res Lett 30(23):2184. DOI 10.1029/2003GL018828

SATREF (2005) SATREF. http://www.satref.no/. Cited June 2005

Scherneck H-G, Vermeer M, Mitrovica JX, Milne GA (2002) BIFROST: Observing the three-dimensional deformation of Fennoscandia. In Ice sheets, sea level and the dynamic earth. Geodynam Ser 29; American Geophysical Union, Washington

SWEPOS (2005) SWEPOS, A national network of reference stations for GPS. http://swepos.lmv.lm.se/english/index.htm. Cited June 2005

Stewart MP, Penna NT, Lichti DD (2005) Investigating the propagation mechanism of unmodelled systematic errors on coordinate time series estimated using least squares. J Geod 79(8):479–489. DOI 10.1007/s00190-005-0478-6

Tregoning P, van Dam T (2005) Effects of atmospheric pressure loading and seven-parameter transformations on estimates of geocenter motion and station heights from space geodetic observations. J Geophys Res 110:B03408. DOI 10.1029/2004JB003334

Watson C, Tregoning P, Coleman R (2006) Impact of solid Earth tide models on GPS coordinate and tropospheric time series. Geophys Res Lett 33:L08306. DOI 10.1029/2005GL025538

Webb F H, Zumberge J F (1993) An introduction to the GIPSY/OASIS-II, Publ. D-11088 Jet Propulsion Laboratory, Pasadena

Wessel P, Smith WHF (1998) New, improved version of Generic Mapping Tools released, EOS Trans Amer Geophys U. 79(47):579

Williams SPD (2003) The effect of coloured noise on the uncertainties of rates estimated from geodetic time series, J Geod 76:483–494. DOI 10.1007/s001990-002-0283-4

Williams SPD, Bock Y, Fang P, Jamason P, Nikolaidis RM, Prawirodirdjo L, Miller M, and Johnson DJ (2004) Error analysis of continuous GPS position time series, J Geophys Res 109, B03412. DOI 10.1029/2003JB002741

Zumberge JF, Heflin MB, Jefferson DC, Watkins MM (1997) Precise point positioning for the efficient and robust analysis of GPS data from large networks. J Geophys Res 102(B3):5005–5017